SEMARAK ILMU
PUBLISHING

CFD *Letters*
ISSN 2810-1363

Identification of Horizontal Gas-Liquid Two-Phase Flow Regime using Deep Learning

Umair Khan[1], William Pao[1,*], Nabihah Sallih[1], Farruk Hassan[2]

[1] Mechanical Engineering Department, Universiti Teknologi PETRONAS (UTP), Seri Iskandar 32610, Malaysia
[2] Computer and Information Sciences Department, High Performance Cloud Computing Centre (HPC3), Universiti Teknologi PETRONAS (UTP), Seri Iskandar 32610, Malaysia

ARTICLE INFO	ABSTRACT
	Two-phase flow is of great importance in various industrial processes. A characteristic feature of two-phase flow is that it can acquire various spatial distribution of phases to form different flow patterns/regimes. The knowledge of flow regime is very important for quantifying the pressure drop, the stability and safety of two-phase flow systems and it holds great significance in petrochemical and thermonuclear industries today. The objective of this study is to develop a methodology for identification of flow regime using dynamic pressure signals and deep learning techniques. Stratified, slug and annular flow regimes were simulated using a Level-Set (LS) method coupled with Volume of Fluid (VOF) method in a 6 m horizontal pipe with 0.050 m inner diameter. Dynamic pressure signals were collected at a strategic location. These signals were converted to scalograms and used as inputs in deep learning architectures like ResNet-50 and ShuffleNet. Both architectures were effective in classifying different flow regime and recorded testing accuracies of 85.7% and 82.9% respectively. According to our knowledge no similar research has been reported in literature, where various Convolutional Neural Networks are used along with dynamic pressure signals to identify flow regime in horizontal pipe. This research provides a benchmark for future research to use dynamic pressure for identification of two-phase flow regimes. This research provides a benchmark for future research to use dynamic pressure for identification of two-phase flow regimes. This study can be extended by collecting data over broader range of flow parameters and different geometries.

1. Introduction

Two-phase flow commonly occurs in oil and gas industries, nuclear power plants and heat exchangers. An important characteristic of two-phase flow is its ability to acquire different spatial arrangements of phases, thus creating different flow patterns. Each pattern has its own hydrodynamic behaviour which influence properties like pressure drop, void fraction, and heat transfer etc. It is very important to identify different flow patterns to avoid destructive phenomenon like flow-induced vibrations and severe slugging [1-3]. Thus, for the successful operation of any two-phase flow system, it is crucial to identify flow pattern. Different flow regime identification methods

---

exist in literature [4-6]. Traditionally, Close Visual Inspection (CVI) was used to determine different flow regimes [7]. This method is highly subjective and only possible for easily accessible transparent pipes, which is not always the case in industries.

Flow regime can also be identified using the fluctuations of natural flow parameters. This approach works on the principle that waveform of these fluctuations is closely related to different flow patterns. Example of such flow regime identification methods are void fraction measured by X-rays, rotating electric field conductance gauge, electrical capacitance tomography, conductivity, and electrical impedance [8-12]. The intrusive nature of some of these methods could alter flow regime change due to sensors placement within the flow stream. Although excellent results can be obtained using radiation techniques, the use of radiation source could lead to health and safety related problems [13].

The use of pressure signals is considered a more practical approach because pressure data is readily available. That is why pressure fluctuations are widely used to identify flow regime [14-19]. Recently, Machine Learning (ML) techniques are used to process pressure and void fraction signals for flow regime identification [20-22]. Mi *et al.,* [12] used void fraction signals to train a neural network and then used the trained network to identify different flow regimes. Wang and Zhang [10] used Support Vector Machine (SVM) to identify different flow patterns by using capacitance signals from Electrical Capacitance Tomography (ECT) system as inputs, Trafalis *et al.,* [23] also used the same method but used superficial velocities and pipe diameter as inputs. Neural networks have also been used to process signals from conductivity probe and vortex flow meters for flow regime identification [11,24].

Most of the literature is based on using differential pressure along with neural networks to identify flow regimes. Differential pressure data needs two pressure readings to be determined at different locations and is a cumbersome process. The present method proposes using dynamic pressure readings which can be obtained at single location. This research also uses deep learning techniques instead of neural networks as classifiers. According to literature, dynamic pressure along with deep learning techniques have never been used before to identify different flow regime in water-air two phase system in horizontal pipe. The difference between traditional and deep learning methods is that the former needs hand crafted features extracted from the time and/or frequency domains to be fed into the ML algorithms, whereas, in deep learning, the Convolutional Neural Networks (CNNs) transform their representation in a more ambiguous manner. Deep learning model automatically learns the hidden patterns in the data. In this study, two different architectures namely ResNet50 and ShuffleNet and compared the performance in terms of classification accuracy.

2. Methodology

The methodology for identification of different flow regimes in two phase flow in a horizontal pipe is discussed in this section. This section will cover the simulation methodology used to collect dynamic pressure signals and neural networks used for classification.

2.1 Geometry

Geometry used in this research is a horizontal pipe with 6 m length and 0.050 m internal diameter. The inlet diameter is divided into air and water inlets as shown in Figure 1. Pressure signals were recorded for a total duration of 10 seconds at 80D from the inlet. From literature flow at this location is expected to be fully developed and thus considered appropriate for data collection [25].
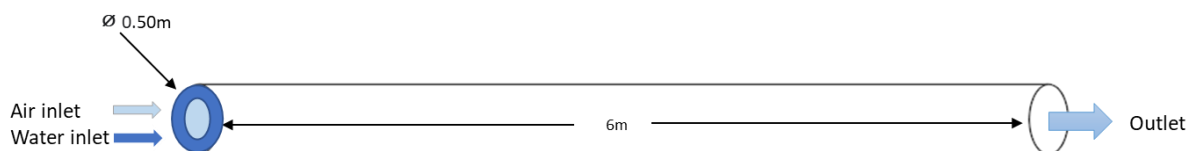
Fig. 1. Geometry of a horizontal pipe used in this study

2.2 Meshing and Mesh Quality Analysis

Hexahedral meshing technique is recommended in literature for two phase flow in pipe and was utilized for mesh generation in ICEM CFD tool [25]. Multizone method was selected to mesh the geometry, as shown in Figure 2. Five Inflation layers were used to capture flow behaviour near the boundary wall accurately, as shown in Figure 2(b).
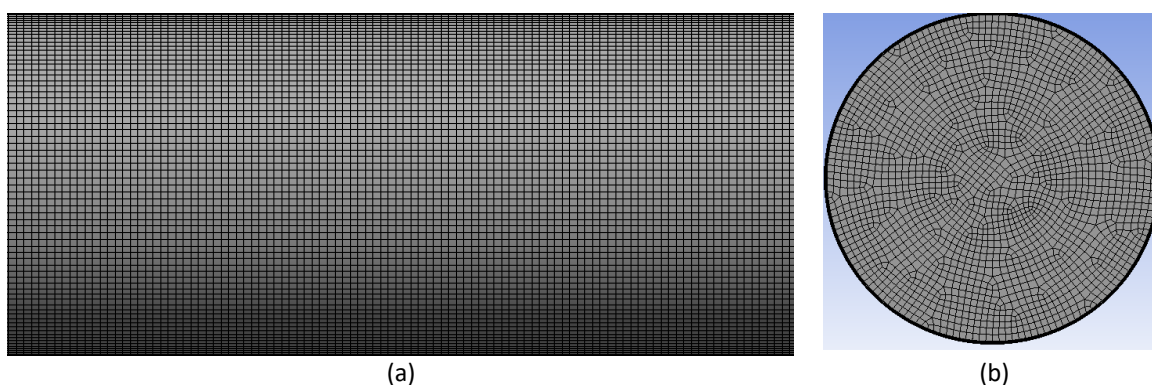
(a)　　　　　　　　　　　　　　　　　　(b)
Fig. 2. Hexahedral mesh (a) horizontal view, and (b) side view showing inlet

The quality of the mesh plays important role in stability and accuracy of numerical solution. The parameters used to check mesh quality are skewness, orthogonal quality, and aspect ratio. Skewness value of 0.12 was recorded in current study. In current study average orthogonal quality was 0.94. The minimum and maximum value of aspect ratio recorded was 1.1 and 8.2. These values are in very good zone for capturing two-phase flow [26].

2.3 Mesh Convergence Study

The performance of numerical studies depends on the selection of proper mesh. The selection of coarse mesh can reduce the accuracy of results while on the other hand selecting very fine mesh can increase cost of simulation. That is why mesh independence study was performed to find the most appropriate mesh size. For this study three meshes were chosen namely coarse, medium, and fine having size of 0.008, 0.005 and 0.004 m respectively as shown in Table 1. During simulation, liquid and gas superficial velocities were kept at 2.0 m/s and 1.8 m/s. Average dynamic pressure at location 80D downstream was calculated.

Table 1
Mesh convergence criteria

Mesh	No. of Elements	Size of Element (m)	Avg. Dynamic Pressure (KPa)
Coarse	175664	0.008	1278
Intermediate	305254	0.005	1218
Fine	458143	0.004	1216

Figure 3 shows the variation in average dynamic pressure for different meshes. When mesh is improved from coarse to medium, the difference between the readings is high which is why coarse mesh is not recommended. In case of changing medium mesh to fine mesh, the difference is negligible. Hence by using fine mesh, number of elements are increased which will increase simulation time and cost, while not improving the results significantly. Hence medium mesh is chosen with number of elements equal to 305254.
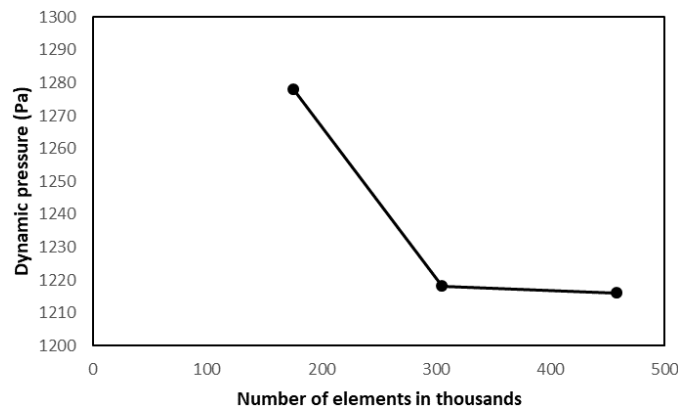
Fig. 3. Mesh dependency study

2.4 Boundary Conditions

The inlet boundary condition was set to be velocity inlet type. Water and gas superficial velocities at inlet were chosen using Taitel and Dukler's [7] flow regime map as shown in Figure 4(b). As shown in the Figure 4(a) both phases were injected separately into the pipe. Gas phase was introduced into the pipe at the centre region while liquid phase was injected peripherally. The boundary condition at outlet was set to outlet pressure which is the value of atmospheric pressure. No slip boundary conditions were set on boundary wall. The atmospheric pressure was used as a reference and isothermal condition was applied. The surface tension of water-air was offset to 0.072 N/m and density of air and water phase used was 998.2 kg/m^3 and 1.225 kg/m^3 respectively.
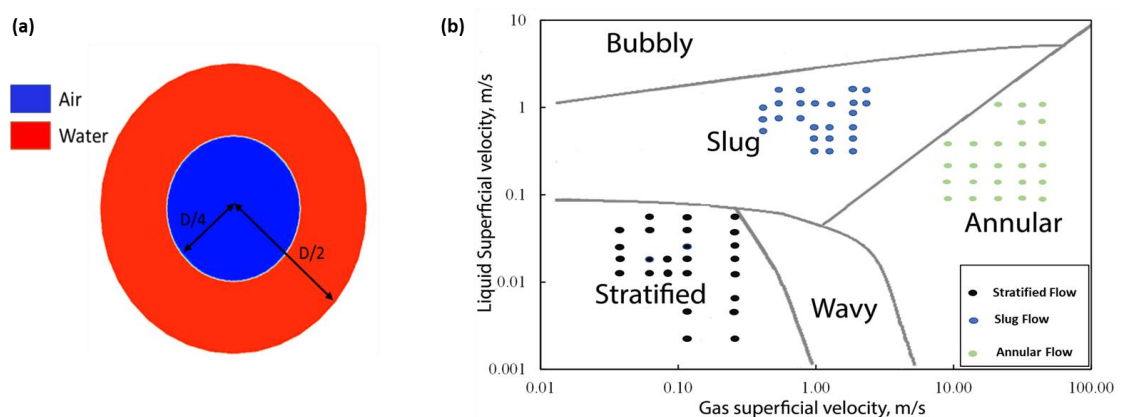
Fig. 4. Boundary Conditions; (a) Air and Water inlet, (b) Water and gas superficial velocities used for simulation of different flow regimes, shown in Taitel and Dukler [7] flow regime map

2.5 Simulation Model

To simulate air-water two phase flow, Level-Set (LS) method coupled with Volume of Fluid (VOF) method is used. Both methods when coupled together, the results are superior compared to standalone VOF or LS method [27]. The continuity and momentum conservation equations for both methods are given by Eq. (1) and Eq. (2), respectively.

$$\frac{\partial \rho}{\partial t} + \nabla \cdot (\rho \mathbf{U}) = 0 \tag{1}$$

$$\frac{\partial}{\partial t}(\rho \mathbf{U}) + \nabla \cdot (\rho \mathbf{U} \otimes \mathbf{U}) = -\nabla p + \nabla \cdot \left[\mu(\nabla \mathbf{U} + \nabla \mathbf{U}^{T}) \right] + \rho \mathbf{g} + \mathbf{F} \tag{2}$$

Where ρ is fluid density, t is time, $\mathbf{U}$ is the fluid velocity vector, p is static pressure, μ is fluid viscosity, $\mathbf{g}$ is the gravitational acceleration and $\mathbf{F}$ represent external body forces.

Realizable k-ϵ model was used for mixture turbulence equations [26]. Governing equations for realizable turbulence model are shown in Eq. (3) and Eq. (4).

$$\frac{\partial}{\partial t}(\rho k) + \nabla \cdot (\rho k \mathbf{U}) = \nabla \cdot \left[\left(\mu + \frac{\mu_t}{\sigma_k} \right) \nabla k \right] + G_k + G_b - \rho_\varepsilon - Y_M + S_k \tag{3}$$

$$\frac{\partial}{\partial t}(\rho \varepsilon) + \nabla \cdot (\rho \mathbf{U} \varepsilon) = \nabla \cdot \left[\left(\mu + \frac{\mu_t}{\sigma_k} \right) \nabla \varepsilon \right] + \rho C_1 S_\varepsilon - \rho C_2 \frac{\varepsilon^2}{k + \sqrt{\upsilon_\varepsilon}} + C_{1\varepsilon} \frac{\varepsilon}{k} C_{3\varepsilon} G_b + S_\varepsilon \tag{4}$$

"Gb" and "Gk" is the turbulence kinetic energy generation due to the buoyancy and mean velocity gradients respectively, "Y_M" is the contribution of dilatation to the overall dissipation rate, "C_1, C_2, $C_{1\varepsilon}$, $C_{3\varepsilon}$" are constants, while σ_k and σ_ε are turbulent Prandtl numbers, Sk and S_ε are user defined source terms [26].

For convergence criteria of simulations, all residuals were set at a value of 10^{-5}. Time step of 0.001s and total physical time of 10s was used. This time step and total time was appropriate to capture nature of different two-phase flow regimes.

2.6 Data Transformation

Continuous Wavelet Transform (CWT) is a tool that captures the time-frequency features of non-stationary signals like pressure signals [28]. The performance of CWT is excellent in the field of signal processing [29]. CWT convert pressure signals to scalogram images which are visual representation of continuous wavelet coefficients as shown in Figure 5. These two-dimensional scalogram images can be used as input for CNN models. A CWT with source wavelet morlet with parameter = 8, was applied to the dynamic pressure signals and scalogram images were obtained, which can be expressed mathematically by Eq. (5). Some examples of scalogram images for different flow regimes are shown in Figure 5.

$$\Psi(\tau) = e^{i\omega_0 \tau} e^{\frac{-\tau^2}{(2\vartheta^2)}} \tag{5}$$

The dilated version of Morlet wavelet in frequency domain is given by Eq. (6).

$$\Psi(\omega) = \vartheta\sqrt{2\pi}e^{\frac{-(a\omega-\omega 0)^2\vartheta^2}{2}} \tag{6}$$

Where ϑ and ω are constants, the wavelet center frequency is denoted by ω_0.
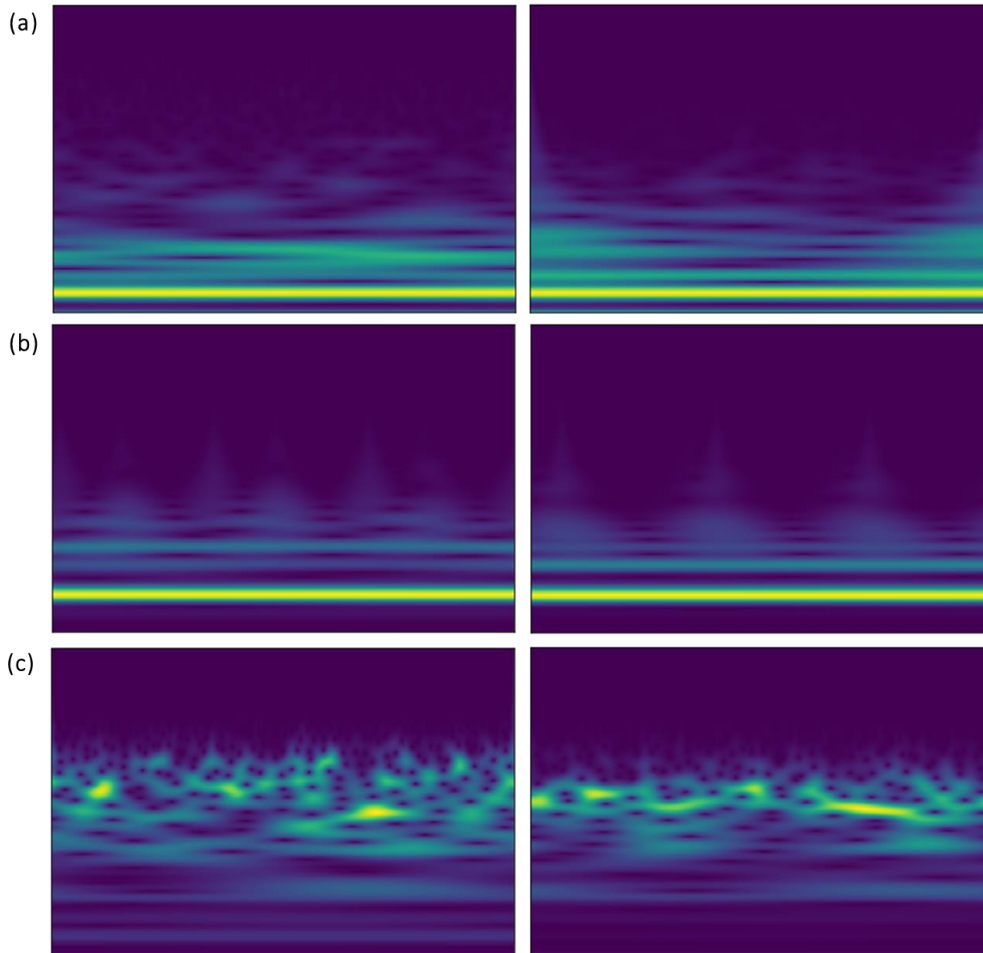
Fig. 5. Scalograms of different flow regimes (a) Stratified flow, (b) Slug flow, (c) Annular flow

2.7 Dataset Preparation

To apply the deep-learning models, pressure scalograms dataset are used as input. The data set was randomly divided into 80/20 training-testing ratios. Twenty percent of the training data were set aside for the validation. There were two deep learning classification architectures used in the experiments, Resnet50 and ShuffleNet. On an Alienware laptop with the following configuration, 16 GB of RAM and an Intel Core i7 2.80 GHz processor with NVIDIA GeForce GTX 1070 GPUs, all the models underwent testing and training. This training was conducted using MATLAB version R2020b.

2.8 Network Architecture

Transfer learning is a technique where a model applied to one machine learning task named A is adapted and used for task B. Transfer learning enhances the performance when modelling the target

task and addresses the issue of limited training data [30]. Pretrained models such as ResNet-50 and ShuffleNet are used to apply transfer learning in this study.

2.8.1 ResNet-50

One of the convolutional neural networks is ResNet-50 architecture which has 50 layers and is a variant of ResNet [31]. It has 48 Convolution layers, one MaxPool and one Average Pool layer. Even with exceedingly deep neural networks, the vanishing gradient problem is resolved. Even though it has 50 layers, Resnet-50 has around 23 million trainable parameters, which is substantially less than other architectures. The explanation for why it performs as it does is still up for debate but explaining residual blocks and how they function will make things clearer. Consider a neural network block where the aim is to learn the true distribution H(x). If its input is x, then the difference between this can be represented as [31]:

$$R(x) = Output - Input = H(x) - x \tag{7}$$

Rearranging it we get,

$$H(x) = R(x) + x \tag{8}$$

The remaining block is attempting to understand the real output, H(x). The layers are learning the residual, R(x), because an identity connection is coming from x.

2.8.2 ShuffleNet

In order to reduce the computation time and fulfil the increasing demand of utilizing effective deep neural networks while keeping accuracy intact, Zhang *et al.,* [32] presented the ShuffleNet model. The model is typically represented by a pointwise group convolution and a channel shuffle operation, which allows more feature map channels to encode more information. Pointwise group convolution is intended to decrease expensive dense 11 convolutions. Since just a tiny portion of the input channel is used to generate the outputs from a given channel, group convolutions degrade representation and block information. Both the networks were trained using the Hyper-parameters given in Table 2.

Table 2
Hyper-parameters used in current study

Hyper-parameter	Value
Optimizer	sgdm
Initial Learning Rate	0.01
Validation Freq	50
L2 Regularization	0.05
MaxEpochs	30
Mini Batch Size	8

3. Results

Two different Convolutional Neural Networks were used to classify three different two-phase flow regimes based on their pressure properties. Figure 6 shows dynamic pressure signals for three different flow regimes. These signals were collected at location 80D from the inlet, for the duration of three seconds. From literature two phase flow is expected to be fully developed at this location [25].
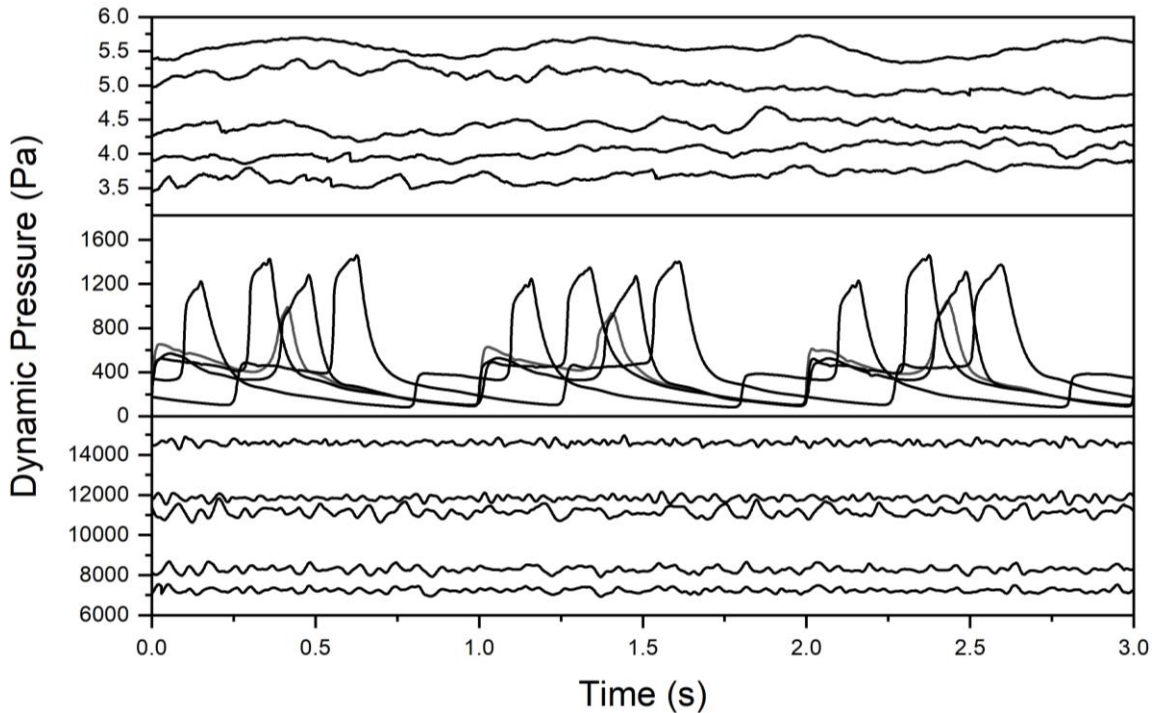
Fig. 6. Dynamic pressure signals: (a) Stratified; (b) Slug; and (c) Annular flow

These dynamic pressure signals are converted into scalograms using CWT, as shown in Figure 5. Scalogram are used for training and testing of Convolutional Neural Networks (CNN). For the classification of different flow regimes, Resnet50 and ShuffleNet architectures were used. The accuracy was chosen as evaluation criteria for both the models. The Resnet50 achieved higher testing accuracy which was 85.7%, while that of ShuffleNet was 82.9%. Both the training and validation losses were recorded. The training and validation loss for Resnet50 was 0.641 and 0.321 respectively, which was higher than ShuffleNet.

Table 3
Performance of ResNet-50 and ShuffleNet architectures

Classifier	Layers	Training Loss	Validation loss	Validation Accuracy	Testing Accuracy
ResNet-50	177	0.641	0.321	94.44	85.7
ShuffleNet	172	0.065	0.166	97.22	82.9

In Figure 7(a), the prediction accuracy for stratified, slug and annular flow regimes are 90.9%, 83.3% and 90.9% respectively. Out of 11 signals for annular flow, Resnet50 correctly identified 10 signals. One of the slug signals was wrongly considered as annular signal. Total number of signals for slug flow were 12 and 10 signals were correctly classified while 1 stratified and 1 annular flow signal was wrongly predicted as slug. In case of stratified flow, 11 signals were used for testing and 10 of them were correctly identified while 1 slug signal was wrongly considered as stratified. In Figure 7(b),

stratified, slug and annular flow regimes were predicted with 83.3%, 83.3% and 81.8% accuracy, respectively. Out of 11 signals for annular flow, ShuffleNet correctly classified 9 signals and one of the slug flows and one stratified flow signal was considered wrongly as annular signal. Total number of signals for slug flow were 13 and 10 signals were correctly classified while 1 stratified and 2 annular flow signals were wrongly predicted as slug. In case of stratified flow, 11 signals were used for testing and 10 of them were correctly identified while 1 slug signals were wrongly considered as stratified.
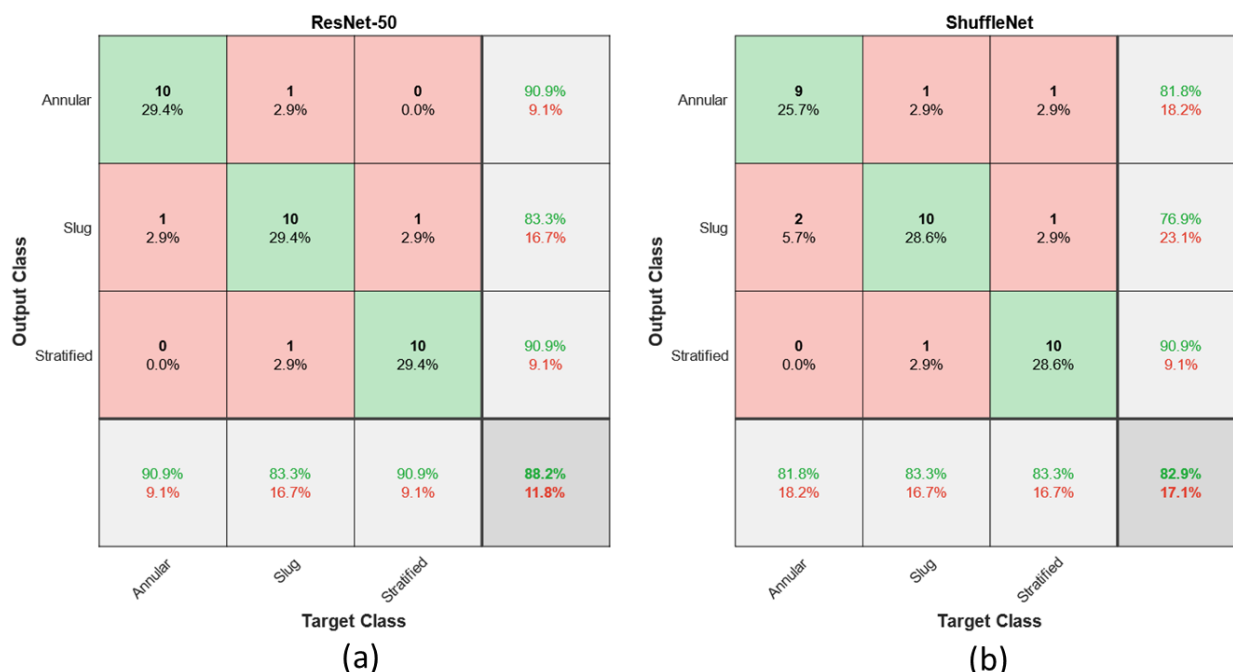
Fig. 7. Confusion matrix of ResNet-50 and ShuffleNet for flow regime classification

4. Conclusions

A method for the identification of gas-liquid two-phase flow regimes in horizontal pipe was developed in this work. This method is based on acquiring dynamic pressure signals and its subsequent scalograms, followed by their classification using Convolutional Neural Networks (CNNs). Tests were conducted to validate and weigh the effectiveness of the proposed identification method. The designed deep learning model has been evaluated against testing dataset. The results showed that the model used has high accuracy in two-phase flow pattern identification. The accuracies of predictions in stratified, slug and annular flows are all above 80%. The Resnet50 achieved higher overall testing accuracy which was 85.7%, while that of ShuffleNet was 82.9%. ResNet50, prediction accuracy for stratified, slug and annular flow regime was 90.9%, 83.3% and 90.9% respectively, while for ShuffleNet stratified, slug and annular flow regimes were predicted with 83.3%, 83.3% and 81.8% accuracy, respectively. Future work should include new experiments with different orientation of pipe, testing broader range of diameters and flow parameters. This work can be taken forward by testing more flow conditions near transition boundaries and defining transition boundaries on flow regime map. More deep learning architectures can be used to check their effect on accuracy.

References

[1] Wang, Yihou, and Nian-Zhong Chen. "An investigation on vortex-induced vibration of a flexible riser transporting severe slugging." *Ocean Engineering* 246 (2022): 110565. https://doi.org/10.1016/j.oceaneng.2022.110565

[2] Hossain, Mamdud, Nkemjika Mirian Chinenye-Kanu, Ghazi Mohamad Droubi, and Sheikh Zahidul Islam. "Investigation of slug-churn flow induced transient excitation forces at pipe bend." *Journal of Fluids and Structures* 91 (2019): 102733. https://doi.org/10.1016/j.jfluidstructs.2019.102733

[3] Khan, Umair, William Pao, and Nabihah Sallih. "A Review: Factors Affecting Internal Two-Phase Flow-Induced Vibrations." *Applied Sciences* 12, no. 17 (2022): 8406. https://doi.org/10.3390/app12178406

[4] Mandhane, J. M., G. A. Gregory, and K. Aziz. "A flow pattern map for gas-liquid flow in horizontal pipes." *International Journal of Multiphase Flow* 1, no. 4 (1974): 537-553. https://doi.org/10.1016/0301-9322(74)90006-8

[5] Kaichiro, Mishima, and Mamoru Ishii. "Flow regime transition criteria for upward two-phase flow in vertical tubes." *International Journal of Heat and Mass Transfer* 27, no. 5 (1984): 723-737. https://doi.org/10.1016/0017-9310(84)90142-X

[6] Shaban, H., and S. Tavoularis. "Identification of flow regime in vertical upward air-water pipe flow using differential pressure signals and elastic maps." *International Journal of Multiphase Flow* 61 (2014): 62-72. https://doi.org/10.1016/j.ijmultiphaseflow.2014.01.009

[7] Taitel, Yemada, and Abe E. Dukler. "A model for predicting flow regime transitions in horizontal and near horizontal gas-liquid flow." *AIChE Journal* 22, no. 1 (1976): 47-55. https://doi.org/10.1002/aic.690220105

[8] Jones Jr, Owen C., and Novak Zuber. "The interrelation between void fraction fluctuations and flow patterns in two-phase flow." *International Journal of Multiphase Flow* 2, no. 3 (1975): 273-306. https://doi.org/10.1016/0301-9322(75)90015-4

[9] Merilo, M., R. L. Dechene, and W. M. Cichowlas. "Void fraction measurement with a rotating electric field conductance gauge." *Journal of Heat Transfer* 99, no. 2 (1977): 330-332. https://doi.org/10.1115/1.3450689

[10] Wang, H. X., and L. F. Zhang. "Identification of two-phase flow regimes based on support vector machine and electrical capacitance tomography." *Measurement Science and Technology* 20, no. 11 (2009): 114007. https://doi.org/10.1088/0957-0233/20/11/114007

[11] Juliá, J. Enrique, Yang Liu, Sidharth Paranjape, and Mamoru Ishii. "Upward vertical two-phase flow local flow regime identification using neural network techniques." *Nuclear Engineering and Design* 238, no. 1 (2008): 156-169. https://doi.org/10.1016/j.nucengdes.2007.05.005

[12] Mi, Y., M. Ishii, and L. H. Tsoukalas. "Vertical two-phase flow identification using advanced instrumentation and neural networks." *Nuclear Engineering and Design* 184, no. 2-3 (1998): 409-420. https://doi.org/10.1016/S0029-5493(98)00212-X

[13] Kreitzer, Paul J., Michael Hanchak, and Larry Byrd. "Horizontal two phase flow regime identification: comparison of pressure signature, electrical capacitance tomography (ECT) and high speed visualization." In *ASME International Mechanical Engineering Congress and Exposition*, vol. 45233, pp. 1281-1291. American Society of Mechanical Engineers, 2012. https://doi.org/10.1115/IMECE2012-89075

[14] Elperin, T., and M. Klochko. "Flow regime identification in a two-phase flow using wavelet transform." *Experiments in Fluids* 32, no. 6 (2002): 674-682. https://doi.org/10.1007/s00348-002-0415-x

[15] Matsui, Goichi. "Automatic identification of flow regimes in vertical two-phase flow using differential pressure fluctuations." *Nuclear Engineering and Design* 95 (1986): 221-231. https://doi.org/10.1016/0029-5493(86)90049-X

[16] Vieira, Saon Crispim, Charlie van der Geest, Adriano Todorovic Fabro, Marcelo Souza de Castro, and Antonio Carlos Bannwart. "Intermittent slug flow identification and characterization from pressure signature." *Mechanical Systems and Signal Processing* 148 (2021): 107148. https://doi.org/10.1016/j.ymssp.2020.107148

[17] Bin, S. U. N., Hongjian Zhang, Lu Cheng, and Z. H. A. O. Yuxiao. "Flow regime identification of gas-liquid two-phase flow based on HHT." *Chinese Journal of Chemical Engineering* 14, no. 1 (2006): 24-30. https://doi.org/10.1016/S1004-9541(06)60033-5

[18] Ali, Farhad, and Nadeem Ahmad Sheikh. "Introductory chapter: Fluid flow problems." In *Fluid Flow Problems*. IntechOpen, 2018. https://doi.org/10.5772/intechopen.81300

[19] Catrawedarma, I. G. N. B., Deendarlianto, and Indarto. "Two phases flow regime assignment based on Wavelet features of pressure signal in the airlift pump-bubble generator." In *AIP Conference Proceedings*, vol. 2403, no. 1, p. 060002. AIP Publishing LLC, 2021. https://doi.org/10.1063/5.0071108

[20] Khan, Umair, William Pao, Nabihah Sallih, and Farruk Hassan. "Flow Regime Identification in Gas-Liquid Two-Phase Flow in Horizontal Pipe by Deep Learning." *Journal of Advanced Research in Applied Sciences and Engineering Technology* 27, no. 1 (2022): 86-91. https://doi.org/10.37934/araset.27.1.8691

[21] Zhang, Yongchao, Amirah Nabilah Azman, Ke-Wei Xu, Can Kang, and Hyoung-Bum Kim. "Two-phase flow regime identification based on the liquid-phase velocity information and machine learning." *Experiments in Fluids* 61, no. 10 (2020): 1-16. https://doi.org/10.1007/s00348-020-03046-x

[22] Nnabuife, Somtochukwu Godfrey, Boyu Kuang, James F. Whidborne, and Zeeshan A. Rana. "Development of gas-liquid flow regimes identification using a noninvasive ultrasonic sensor, belt-shape features, and convolutional neural network in an s-shaped riser." *IEEE Transactions on Cybernetics* (2021). https://doi.org/10.1109/TCYB.2021.3084860

[23] Trafalis, Theodore B., Olutayo Oladunni, and Dimitrios V. Papavassiliou. "Two-phase flow regime identification with a multiclassification support vector machine (SVM) model." *Industrial & Engineering Chemistry Research* 44, no. 12 (2005): 4414-4426. https://doi.org/10.1021/ie048973l

[24] Sun, Zhiqiang, and Hongjian Zhang. "Neural networks approach for prediction of gas-liquid two-phase flow pattern based on frequency domain analysis of vortex flowmeter signals." *Measurement Science and Technology* 19, no. 1 (2007): 015401. https://doi.org/10.1088/0957-0233/19/1/015401

[25] Ban, Sam, William Pao, and Mohammad Shakir Nasif. "Numerical simulation of two-phase flow regime in horizontal pipeline and its validation." *International Journal of Numerical Methods for Heat & Fluid Flow* 28, no. 6 (2018): 1279-1314. https://doi.org/10.1108/HFF-05-2017-0195

[26] Fluent, A.N.S.Y.S. "ANSYS fluent theory guide 15.0." *ANSYS, Canonsburg, PA 33* (2013).

[27] Nichita, Bogdan A., Iztok Zun, and John R. Thome. "A level set method coupled with a volume of fluid method for modeling of gas-liquid interface in bubbly flow." *Journal of Fluids Engineering* 132, no. 8 (2010): 081302. https://doi.org/10.1115/1.4002166

[28] Gou, Linfeng, Huihui Li, Hua Zheng, Huacong Li, and Xiaoning Pei. "Aeroengine control system sensor fault diagnosis based on CWT and CNN." *Mathematical Problems in Engineering* 2020 (2020). https://doi.org/10.1155/2020/5357146

[29] Pacheco-Chérrez, Josué, Diego Cárdenas, and Oliver Probst. "Experimental Detection and Measurement of Crack-Type Damage Features in Composite Thin-Wall Beams Using Modal Analysis." *Sensors* 21, no. 23 (2021): 8102. https://doi.org/10.3390/s21238102

[30] Olivas, Emilio Soria, Jos David Mart Guerrero, Marcelino Martinez-Sober, Jose Rafael Magdalena-Benedito, and L. Serrano, eds. *Handbook of research on machine learning applications and trends: Algorithms, methods, and techniques: Algorithms, methods, and techniques*. Information Science Reference, 2009. https://doi.org/10.4018/978-1-60566-766-9

[31] He, Kaiming, Xiangyu Zhang, Shaoqing Ren, and Jian Sun. "Deep residual learning for image recognition." In *Proceedings of the IEEE Conference on Computer Vision and Pattern Recognition*, pp. 770-778. 2016. https://doi.org/10.1109/CVPR.2016.90

[32] Zhang, Xiangyu, Xinyu Zhou, Mengxiao Lin, and Jian Sun. "ShuffleNet: An extremely efficient convolutional neural network for mobile devices." In *Proceedings of the IEEE Conference on Computer Vision and Pattern Recognition*, pp. 6848-6856. 2018. https://doi.org/10.1109/CVPR.2018.00716